**Reagents**

ATV sulfate was obtained from Gyma Laboratories of America Inc. (Westbury, NY) and free-based with triethylamine. Freebase RTV was acquired from Shengda Pharmaceutical Co. (Zhejiang, China). Poloxamer 407 (P407), FA and CF568-succinimidyl ester (CF568) were purchased from Sigma-Aldrich (St. Louis, MO). CF633-succinimidyl ester (CF633) was purchased from Biotium, Hayward, CA. URMC-099 was synthesized and provided by Califla Bio Inc. (San Diego, CA). Rab5, -7, -11 and -14 antibodies (rabbit anti-human), HRP-conjugated goat anti-rabbit IgG and Alexa Fluor 488 goat anti-rabbit IgG were purchased from Santa Cruz Biotechnology (Dallas, TX). CD3 antibody (Abcam, Cambridge, MA), CD45 and HIV-1p24 antibodies (Dako, Carpinteria, CA) were used. Puregene Core Kit A and RNeasy mini kit were purchased from Qiagen (Valencia, CA). Macrophage colony stimulating factor (MCSF) was prepared from 5/9m alpha3-18 cells (ATCC®, CRL-10154™). Benzonase® Nuclease was purchased from Merck KGaA (Darmstadt, Germany).

**Preparation of nanoformulated ATV/r**

Nanoformulations of ATV and ritonavir (r) were prepared by high-pressure homogenization (Avestin EmulsiFlex-C3, Avestin Inc., Ottawa, ON, Canada). For preparation of FA-nanoATV/r, free-base ATV or ritonavir (1% w/v), P407 (0.3%, w/v) and FA-P407 (0.2% w/v) were suspended in 10 mM HEPES, pH 7.8, and mixed overnight. For preparation of nanoATV, P407 (0.5%, w/v) and free-base ATV (1%, w/v) were suspended in 10 mM HEPES, pH 7.8 and mixed overnight. The suspensions were homogenized at 20,000 psi until the desired particle size was achieved (300-400 nm).

Particle size, polydispersity and surface charge (zeta potential) were determined by dynamic light scattering using a Malvern Zetasizer Nano ZS (Malvern Instruments Inc., Westborough, MA). Drug loading of the nanoparticles was determined by HPLC with UV/Vis detection. Fluorescently-labeled nanoART was prepared and purified using CF568-modified P407 or CF633-modified P188 as described previously [15]. Characteristics of the nanoformulations are shown in Supplementary Table 1.

**Supplementary Table 1. Characterization of nanoART.**

| Formulation | Size | Zeta-potential | PDI |
|---|---|---|---|
| nanoATV | 371 ± 10 nm | -28 ± 3 mV | 0.19 ± 0.01 |
| FA-nanoATV | 374 ± 3 nm | -14 ± 1 mV | 0.23 ± 0.01 |
| FA-nanoRTV | 390 ± 22 nm | -6 ± 10 mV | 0.21 ± 0.01 |

**Generation of CD34+ mice and HIV-1 infection**

Briefly, fetal liver tissue was used to isolate CD34+ cells by immunomagnetic bead method (Miltenyi Biotec Inc., Auburn, CA). Sublethally irradiated newborn NSG mice were injected intrahepatically with $10^6$ CD34+ cells. After 22-26 weeks, healthy mice were selected and infected intraperitoneally with HIV-$1_{ADA}$ at $10^4$ $TCID_{50}$/mouse. Mice were bled from facial vein before infection, 9 weeks after HIV-1 infection and peripheral blood was analyzed for human CD45 and T cells (CD3, CD4 and CD8) by flow cytometry. Plasma VL was determined using an automated COBAS Amplicor System v1.5 (Roche Molecular Diagnostics, Basel, Switzerland). Mice were placed on folate-deficient diet (Harlan Teklad TD.00434, Harlan Laboratories, Indianapolis, IN) from 14 days prior to drug administration to the end of the study.

**Immunohistochemistry**

Immunohistochemistry on Spleen and lymph nodes were fixed in 4% paraformaldehyde overnight. Paraffin embedded 5 mm thick adjacent sections were obtained and stained for human cells and HIV-1 virus with monoclonal antibodies to human CD45, HLA-DR and HIV-1p24. An HRP-conjugated secondary antibody to mouse IgG was used and developed with 3,3′-diaminobenzidine. Images were captured using a Nikon DS-Fi1 camera fixed to a Nikon Eclipse E800 (Nikon Instruments, Melville, NY). Spleen sections were double stained for human T-cells and HIV-1 with rabbit anti-human CD3 and mouse anti-HIV-1p24 antibodies. Sections were also double stained with mouse monoclonal antibodies to human macrophages (CD68) and rabbit anti-human Rab7 antibodies. Alex Fluor 594/488-anti-mouse IgG-, alex Fluor 488--anti-rat Ig Gand goat Alex Fluor 488/594-anti-rabbit IgG were used as secondary antibodies in different combinations. Immunofluorescence staining was captured using a LSM 510 confocal microscope (Carl Zeiss Microimaging Inc., Dublin, CA) or Nuance microscopy for quantifications as described [6].

**Monocyte-macrophage cultures**

Cells were cultured in Dulbecco's Modified Eagle's Medium (DMEM) (Invitrogen, Grand Island, NY) with 10% heat-inactivated pooled human serum, 2 mM L-glutamine, 50 mg/ml gentamicin, 10 mg/ml ciprofloxacin and 1000 U/ml MCSF and maintained at 37° C in a 5% $CO_2$ incubator for 7 days to facilitate differentiation into MDM.

**Confocal Microscopy**

Tissues were collected from BALB/c mice 12 hours-post IP injection with 100 mg/ kg CF633-labeled nanoATV and flash-frozen in Tissue-Tek O.C.T. Compound (Optimal Cutting Temperature) using dry ice. Following cryogenic sectioning, tissues were fixed in 3.7% formaldehyde for 15-20 minutes permeabilized in 0.5% Triton X-100 for 5-7 minutes and blocked for 30 minutes in 5% BSA solution. Tissues were incubated with rat anti-F4/80 (abcam, Cambridge, MA) at a 1:100 dilution in 2.5% BSA for 1 hour followed by incubation with Alexa Fluor 488 goat anti-rat (Life Technologies-Molecular Probes, Grand Island, NY) at a 1:100 dilution for 1 hour. Immunofluorescence was evaluated with Zeiss LSM710 confocal microscope using Zen 2011 software (Carl Zeiss Microimaging Inc., Thornwood, NY).

**Western blots**

Treated MDM were lysed in 5 mM Tris-HCl (pH 8.0) containing 0.1% Tween X-100 (Sigma-Aldrich) and Halt protease inhibitor cocktail (1:100 dilution, v/v) (Thermo Scientific, Rockford IL). Protein concentrations were determined using the Micro BCA Protein Assay kit (Thermo Scientific, Rockford, IL). Proteins were separated by gel electrophoresis on a 15% SDS-polyacrylamide gel and immunoblotted to a PVDF membrane. Membrane was blocked with 5% non-fat dry milk in PBS and probed with Rab5, 7, LAMP1 or STAT1 primary antibody (Santa Cruz Biotechnology, Santa Cruz, CA) overnight at 4 °C, followed by incubation with HRP-conjugated secondary antibody (Santa Cruz Biotechnology) for 1 hour at room temperature. Chemiluminoscent signals

were detected and analyzed using FluorChem M system (Proteinsimple, Santa Clara, CA).

**HIV-1p24 immunostaining**

HIV-1 p24 staining was performed as described and details are provided in supplement. For HIV-1p24 immunofluorescence staining [29], MDM were fixed in 4% ice-cold PFA in PBS for 30 min. Fixed cells were washed with PBS and permeabilized in 0.5% Triton X-100 in PBS for 15 min at room temperature. Cells were blocked using 5% goat serum in PBS for 30 min and incubated with mouse monoclonal antibody to HIV-1p24 (DAKO). Alex Fluor 593-conjugated secondary antibody was used to detect HIV-1p24 antigen. Immunofluorescence staining was quantified using Nuance software (Cambridge Research & Instrumentation, Boston, MA).

**MDM nanoATV uptake and retention**

MDM were treated with 100 $\mu$M nanoATV alone or in the presence of 10 ng/ml URMC-099 for 16 hours. The cells were collected at multiple time points (1, 4, 8 and 16 hours). After drug loading MDM were washed with PBS, and fresh medium was added with or without 10 ng/ml URMC-099. Cells were collected at 0, 1, 5, 10 or 15 days for isolation of endosomal compartments and nanoATV retention. Immunoisolation of endocytic compartments was performed as previously described [30]. Briefly, cells were washed 3 times with ice-cold PBS and scraped into homogenization buffer (10 mM HEPES-KOH, pH 7.2, 250 mM sucrose, 1 mM EDTA, and 1 mM $Mg(OAc)_2$). Cells were disrupted by 15 strokes in a Dounce homogenizer. Cell homogenates were centrifuged at 400 × *g* for

10 min at 4 °C to remove the unbroken cells and nuclei. Twenty $\mu$L of slurry protein A/G paramagnetic beads conjugated to Rab5, -7 or -11 (binding in 10% BSA in PBS for 12 hours at 4 °C) were incubated with cell supernatants for 24 hours at 4 °C. Endocytic compartments were washed with PBS and collected by magnetic separation for 1 hour at 4 °C. ATV content in isolated endosomal fractions was quantitated by HPLC as previously described [30].

**Supplementary Figures**

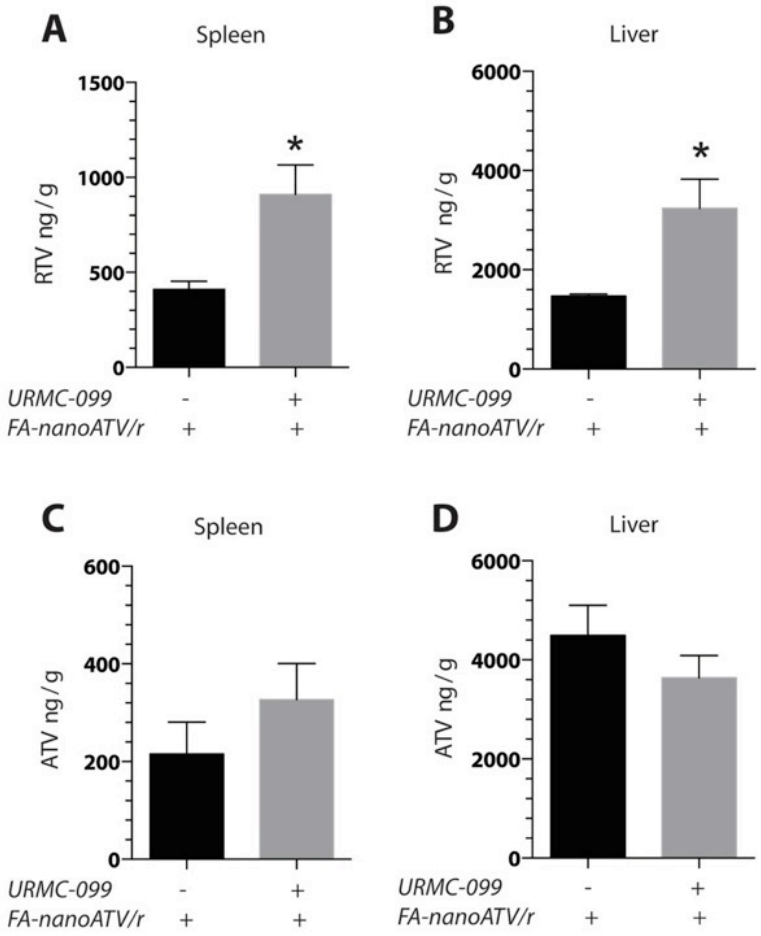


**Figure S1. URMC-099 effects on FA-nanoATV/r drug levels in humanized HIV-$1_{ADA}$-infected CD34+ NSG mice.** Ten weeks after infection mice were treated with daily IP injection of 10 mg/kg URMC-099 with or without weekly intramuscular administration of 100 mg/kg FA-nanoATV/r. Three weeks after treatment, UPLC-MS/MS determined drug levels. RTV and ATV drug concentrations in spleen (A and C) and liver (B and D) are shown. Data are expressed as average $\pm$ SEM of n = 5 ($p < 0.05$, paired 2-tailed t-test). *Different from FA-nanoATV/r treatment.

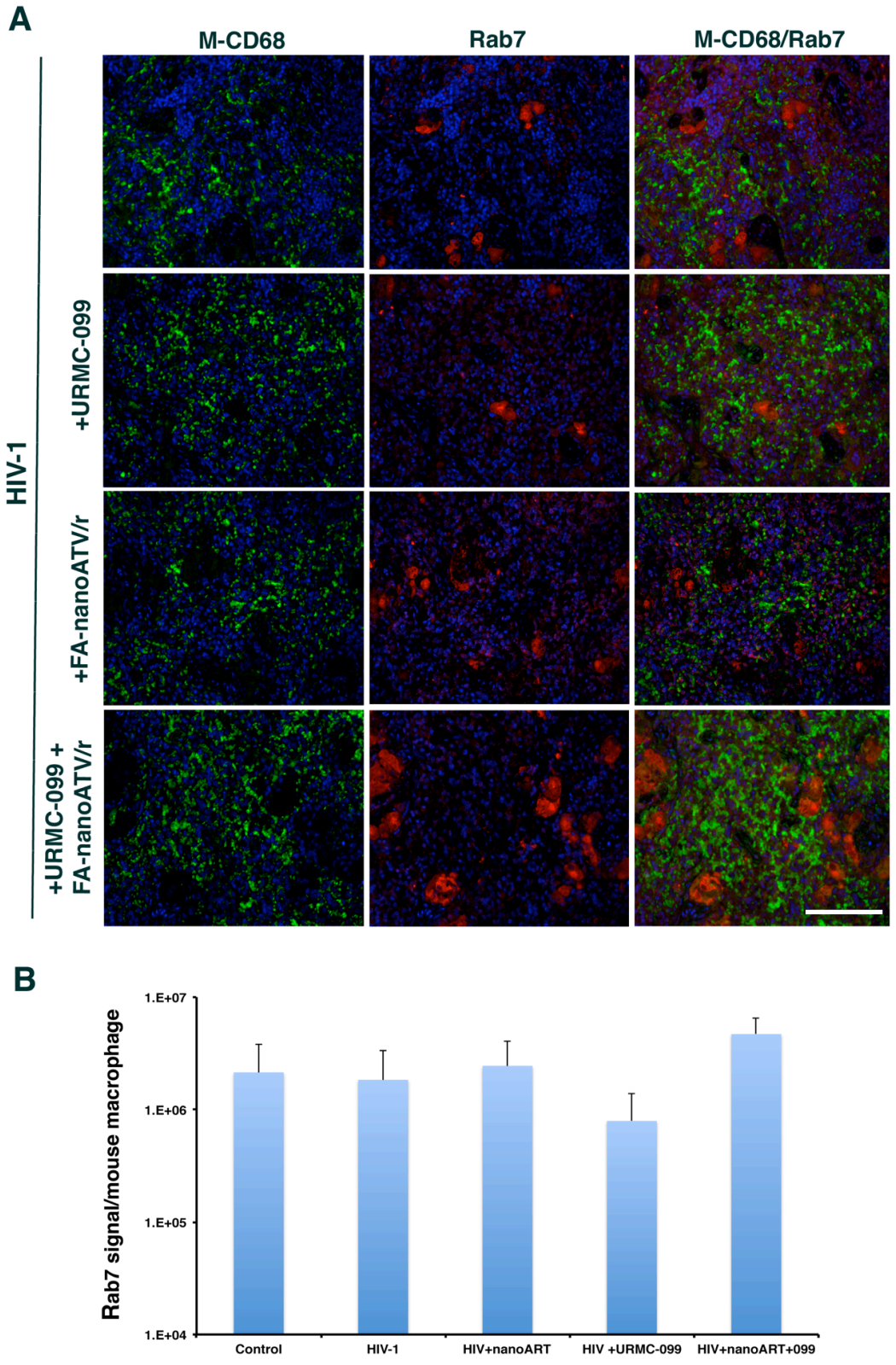
A
M-CD68
Rab7
M-CD68/Rab7
HIV-1
+URMC-099
+FA-nanoATV/r
+URMC-099 +
FA-nanoATV/r
B
Rab7 signal/mouse macrophage
1.E+07
1.E+06
1.E+05
1.E+04
Control
HIV-1
HIV+nanoART
HIV +URMC-099
HIV+nanoART+099

**Figure S2. Immunofluorescence double staining of mouse macrophages** (CD68-green) and human Rab7 (Red), (A) showing almost identical expression of co-localized Rab7 in mouse macrophages in HIV-1 infected, infected and FA-nanoATV/r treated, double treatment group as compared to control animals (B) immunofluorescence quantification of tissue sections from the above treatment group. We observe a significant decrease in expression only in URMC-099 treated animals as compared to the FA-nanoART and FA-nanoART and URMC-099 double treatment group ($p < 0.05$, 03 respectively). Scale bar equals 50$\mu$m.

**A**

| Accession | UniprotID | Z test | Z test_pval | Accession | UniprotID | Z test | Z test_pval |
|---|---|---|---|---|---|---|---|
| O94979 | SC31A_HUMAN | 1.970992604 | 0.048724722 | P51149 | RAB7A_HUMAN | 2.705351213 | 0.006823221 |
| Q13347 | EIF3I_HUMAN | 1.978401522 | 0.047883428 | Q00341 | VIGLN_HUMAN | 2.712492269 | 0.006677934 |
| P31040 | DHSA_HUMAN | 1.982994363 | 0.047368059 | P00813 | ADA_HUMAN | 2.715781648 | 0.006611951 |
| Q9H444 | CHM4B_HUMAN | 1.983384485 | 0.047324499 | Q13045 | FLII_HUMAN | 2.723439633 | 0.006460602 |
| P26640 | SYVC_HUMAN | 1.98905371 | 0.046695275 | P16989 | YBOX3_HUMAN | 2.72690434 | 0.006393157 |
| P04003 | C4BPA_HUMAN | 2.000681099 | 0.045426768 | P42224 | STAT1_HUMAN | 2.741993988 | 0.006106746 |
| O96011 | PX11B_HUMAN | 2.003708852 | 0.045101257 | P10909 | CLUS_HUMAN | 2.743882935 | 0.006071719 |
| P35914 | HMGCL_HUMAN | 2.005904019 | 0.044866489 | P47897 | SYQ_HUMAN | 2.746041976 | 0.006031905 |
| P98171 | RHG04_HUMAN | 2.015587021 | 0.043843178 | Q9Y5M8 | SRPRB_HUMAN | 2.775330845 | 0.005514558 |
| Q96QK1 | VPS35_HUMAN | 2.019923068 | 0.043391368 | Q9H0U3 | MAGT1_HUMAN | 2.78970448 | 0.005275617 |
| Q9H4A6 | GOLP3_HUMAN | 2.020501116 | 0.043331435 | Q14789 | GOGB1_HUMAN | 2.813095625 | 0.004906706 |
| P18085 | ARF4_HUMAN | 2.024306917 | 0.042938582 | Q68EM7 | RHG17_HUMAN | 2.81886822 | 0.00481933 |
| O43464 | HTRA2_HUMAN | 2.030208911 | 0.042335308 | P30419 | NMT1_HUMAN | 2.842412734 | 0.004477349 |
| Q8NHM4 | TRY6_HUMAN | 2.031272989 | 0.04222731 | P62820 | RAB1A_HUMAN | 2.845508325 | 0.00443406 |
| P83731 | RL24_HUMAN | 2.031477546 | 0.042206575 | Q9Y4K1 | AIM1_HUMAN | 2.857101977 | 0.004275285 |
| Q9H0E2 | TOLIP_HUMAN | 2.036410582 | 0.041709144 | Q13263 | TIF1B_HUMAN | 2.865245602 | 0.004166859 |
| Q02318 | CP27A_HUMAN | 2.042937283 | 0.041058647 | Q9NP72 | RAB18_HUMAN | 2.872257349 | 0.004075509 |
| Q99439 | CNN2_HUMAN | 2.045551948 | 0.040800473 | Q9Y3I0 | RTCB_HUMAN | 2.877237827 | 0.004011731 |
| P02649 | APOE_HUMAN | 2.063715269 | 0.039044721 | Q658P3 | STEA3_HUMAN | 2.898991428 | 0.003743651 |
| O43837 | IDH3B_HUMAN | 2.103231133 | 0.03544557 | Q9Y4I1 | MYO5A_HUMAN | 2.936366796 | 0.003320814 |
| Q9H3Z4 | DNJC5_HUMAN | 2.119376745 | 0.034058641 | P16435 | NCPR_HUMAN | 2.982869338 | 0.002855599 |
| P35637 | FUS_HUMAN | 2.120740886 | 0.033943614 | P48147 | PPCE_HUMAN | 3.007994979 | 0.002629775 |
| Q13459 | MYO9B_HUMAN | 2.128048194 | 0.033333088 | Q9GZT3 | SLIRP_HUMAN | 3.037858428 | 0.002382659 |
| P60866 | RS20_HUMAN | 2.129417197 | 0.033219759 | Q9ULV4 | COR1C_HUMAN | 3.122086334 | 0.001795743 |
| Q9HD20 | AT131_HUMAN | 2.140007532 | 0.032354158 | Q07020 | RL18_HUMAN | 3.123773577 | 0.001785478 |
| P36776 | LONM_HUMAN | 2.140498745 | 0.032314482 | Q8N5M1 | ATPF2_HUMAN | 3.134062989 | 0.001724038 |
| P11233 | RALA_HUMAN | 2.140640683 | 0.032303025 | O15143 | ARC1B_HUMAN | 3.148005379 | 0.001643887 |
| Q9BUF5 | TBB6_HUMAN | 2.144702213 | 0.031976664 | O75396 | SC22B_HUMAN | 3.164563358 | 0.001553158 |
| P26440 | IVD_HUMAN | 2.153915747 | 0.03124678 | O75369 | FLNB_HUMAN | 3.188346747 | 0.001430888 |
| Q5TEJ8 | THMS2_HUMAN | 2.158112554 | 0.030919082 | P33176 | KINH_HUMAN | 3.199657753 | 0.001375909 |
| Q99541 | PLIN2_HUMAN | 2.162162138 | 0.030605681 | Q9H4G4 | GAPR1_HUMAN | 3.217832349 | 0.001291633 |
| Q9H3P7 | GCP60_HUMAN | 2.164491573 | 0.030426643 | Q14498 | RBM39_HUMAN | 3.226958617 | 0.001251136 |
| Q5JWF2 | GNAS1_HUMAN | 2.16681456 | 0.030248997 | P48668 | K2C6C_HUMAN | 3.235627845 | 0.001213755 |
| Q04637 | IF4G1_HUMAN | 2.175650733 | 0.029581387 | Q9BWF3 | RBM4_HUMAN | 3.238653434 | 0.001200954 |
| Q15691 | MARE1_HUMAN | 2.189026963 | 0.02859488 | P35527 | K1C9_HUMAN | 3.248850252 | 0.001158725 |
| P21283 | VATC1_HUMAN | 2.202750593 | 0.027612332 | P31943 | HNRH1_HUMAN | 3.295409559 | 0.000982783 |
| P40939 | ECHA_HUMAN | 2.208300982 | 0.027223299 | O95470 | SGPL1_HUMAN | 3.32010982 | 0.00089982 |
| P49327 | FAS_HUMAN | 2.212877168 | 0.026906115 | P08779 | K1C16_HUMAN | 3.32766994 | 0.000875756 |
| P10515 | ODP2_HUMAN | 2.243630569 | 0.024856181 | Q03252 | LMNB2_HUMAN | 3.348506019 | 0.000812485 |
| Q9NZ01 | TECR_HUMAN | 2.250512808 | 0.024416411 | P46783 | RS10_HUMAN | 3.360975534 | 0.000776677 |
| Q96JB5 | CK5P3_HUMAN | 2.250852388 | 0.024394888 | Q9Y394 | DHRS7_HUMAN | 3.363825532 | 0.000768701 |
| Q5K4L6 | S27A3_HUMAN | 2.255552525 | 0.024098669 | P33121 | ACSL1_HUMAN | 3.460586705 | 0.000539 |
| Q7Z2K6 | ERMP1_HUMAN | 2.262310319 | 0.023678237 | Q15738 | NSDHL_HUMAN | 3.50763162 | 0.000452115 |
| O60763 | USO1_HUMAN | 2.264719918 | 0.023529872 | P62753 | RS6_HUMAN | 3.551258855 | 0.000383393 |
| Q0VD83 | APOBR_HUMAN | 2.26532872 | 0.023492515 | Q9BPW9 | DHRS9_HUMAN | 3.660622529 | 0.000251603 |
| Q6ICG6 | K0930_HUMAN | 2.298004173 | 0.021561552 | P36542 | ATPG_HUMAN | 3.66942955 | 0.000243092 |
| O15145 | ARPC3_HUMAN | 2.298728054 | 0.021520386 | Q03518 | TAP1_HUMAN | 3.786795079 | 0.000152603 |
| P05771 | KPCB_HUMAN | 2.312650134 | 0.020741883 | Q9BXS5 | AP1M1_HUMAN | 3.798548941 | 0.000145546 |
| P38646 | GRP75_HUMAN | 2.317363194 | 0.020483956 | Q13200 | PSMD2_HUMAN | 3.87175903 | 0.000108053 |
| P22307 | NLTP_HUMAN | 2.318048753 | 0.020446672 | O60841 | IF2P_HUMAN | 4.000616436 | 6.31777E-05 |
| Q16181 | SEPT7_HUMAN | 2.323391058 | 0.020158154 | O95232 | LC7L3_HUMAN | 4.021136563 | 5.7918E-05 |
| Q9Y4P3 | TBL2_HUMAN | 2.333115271 | 0.019642096 | P31948 | STIP1_HUMAN | 4.132684675 | 3.5855E-05 |
| P22626 | ROA2_HUMAN | 2.338991573 | 0.01933587 | P04792 | HSPB1_HUMAN | 4.155323289 | 3.24828E-05 |
| P51648 | AL3A2_HUMAN | 2.345575018 | 0.018997755 | Q7Z2W4 | ZCCHV_HUMAN | 4.221791022 | 2.42369E-05 |
| P21333 | FLNA_HUMAN | 2.354648985 | 0.01854021 | P38606 | VATA_HUMAN | 4.316528546 | 1.58502E-05 |
| O75131 | CPNE3_HUMAN | 2.357627356 | 0.018392145 | P20592 | MX2_HUMAN | 4.563301757 | 5.03554E-06 |
| O15258 | RER1_HUMAN | 2.365216563 | 0.01801953 | P29590 | PML_HUMAN | 4.599399456 | 4.23711E-06 |
| Q9BSJ8 | ESYT1_HUMAN | 2.371767837 | 0.017703211 | Q969G3 | SMCE1_HUMAN | 4.608953552 | 4.04701E-06 |
| Q96HY6 | DDRGK_HUMAN | 2.387544064 | 0.016961369 | P14317 | HCLS1_HUMAN | 4.654082744 | 3.25426E-06 |
| O95721 | SNP29_HUMAN | 2.3998851 | 0.016400219 | P48047 | ATPO_HUMAN | 4.657396082 | 3.20234E-06 |
| P46459 | NSF_HUMAN | 2.42104018 | 0.015476167 | P43307 | SSRA_HUMAN | 4.661772698 | 3.13497E-06 |
| P33897 | ABCD1_HUMAN | 2.430051252 | 0.015096688 | P62847 | RS24_HUMAN | 4.780956898 | 1.74463E-06 |
| Q15149 | PLEC_HUMAN | 2.437029029 | 0.014808491 | P55084 | ECHB_HUMAN | 4.843824078 | 1.27364E-06 |
| Q6NYC8 | PPR18_HUMAN | 2.453175781 | 0.014160112 | Q9H1C7 | CYTM1_HUMAN | 4.924876814 | 8.44135E-07 |
| P30038 | AL4A1_HUMAN | 2.465487982 | 0.013682676 | Q8NHL6 | LIRB1_HUMAN | 4.965674107 | 6.84628E-07 |
| Q53EU6 | GPAT3_HUMAN | 2.486735162 | 0.012892133 | P13647 | K2C5_HUMAN | 5.019617102 | 5.17746E-07 |
| Q9NTJ5 | SAC1_HUMAN | 2.488320871 | 0.012834788 | P51659 | DHB4_HUMAN | 5.045978565 | 4.51206E-07 |
| Q16822 | PCKGM_HUMAN | 2.490458308 | 0.012757846 | O60488 | ACSL4_HUMAN | 5.204256049 | 1.94775E-07 |
| O60784 | TOM1_HUMAN | 2.514813341 | 0.011909542 | Q14247 | SRC8_HUMAN | 5.204525837 | 1.94493E-07 |
| P35908 | K22E_HUMAN | 2.514958957 | 0.011904624 | P48681 | NEST_HUMAN | 5.22666135 | 1.72598E-07 |
| O15270 | SPTC2_HUMAN | 2.526232067 | 0.011529329 | Q12874 | SF3A3_HUMAN | 5.238149732 | 1.62194E-07 |
| P13645 | K1C10_HUMAN | 2.536246942 | 0.011204769 | P27816 | MAP4_HUMAN | 5.367293279 | 7.9927E-08 |
| Q9NQL2 | RRAGD_HUMAN | 2.549716444 | 0.010781057 | Q9C0E8 | LNP_HUMAN | 5.436707973 | 5.4274E-08 |
| Q6ZSR9 | YJ005_HUMAN | 2.556323893 | 0.01057846 | P62854 | RS26_HUMAN | 5.765173431 | 8.15739E-09 |
| P08107 | HSP71_HUMAN | 2.570093575 | 0.010167105 | P69905 | HBA_HUMAN | 5.781441892 | 7.40631E-09 |
| Q96I24 | FUBP3_HUMAN | 2.570380801 | 0.010158678 | Q32MZ4 | LRRF1_HUMAN | 6.163219983 | 7.12804E-10 |
| P19878 | NCF2_HUMAN | 2.580862137 | 0.009855393 | Q9UI12 | VATH_HUMAN | 6.168852036 | 6.87876E-10 |
| P42765 | THIM_HUMAN | 2.585990152 | 0.0097097 | Q9UHD8 | SEPT9_HUMAN | 6.30863266 | 2.81511E-10 |
| P18031 | PTN1_HUMAN | 2.62472101 | 0.008671999 | Q92499 | DDX1_HUMAN | 6.434513694 | 1.23869E-10 |
| O60749 | SNX2_HUMAN | 2.626488184 | 0.008627099 | Q96FZ7 | CHMP6_HUMAN | 6.556484473 | 5.5091E-11 |
| P04264 | K2C1_HUMAN | 2.626930368 | 0.008615896 | Q14005 | IL16_HUMAN | 6.792455828 | 1.10241E-11 |
| Q9Y679 | AUP1_HUMAN | 2.64914608 | 0.008069544 | P40616 | ARL1_HUMAN | 6.89801284 | 5.27356E-12 |
| Q14204 | DYHC1_HUMAN | 2.650773162 | 0.008030776 | P21281 | VATB2_HUMAN | 7.09764349 | 1.26898E-12 |
| Q9H7F0 | AT133_HUMAN | 2.654648046 | 0.007939119 | P41091 | IF2G_HUMAN | 7.515383018 | 5.68434E-14 |
| P52272 | HNRPM_HUMAN | 2.664279471 | 0.007715344 | P11940 | PABP1_HUMAN | 8.085553514 | 6.66134E-16 |
| P53621 | COPA_HUMAN | 2.668973233 | 0.007608351 | Q99536 | VAT1_HUMAN | 8.258364475 | 2.22045E-16 |
| P31937 | 3HIDH_HUMAN | 2.675066433 | 0.007471444 | Q9UQ35 | SRRM2_HUMAN | 8.411408778 | 0 |
| Q9BZQ8 | NIBAN_HUMAN | 2.679847961 | 0.007365561 | Q9Y6N5 | SQRD_HUMAN | 9.893130873 | 0 |
| O60826 | CCD22_HUMAN | 2.695966973 | 0.007018463 | Q9Y6G9 | DC1L1_HUMAN | 10.85909975 | 0 |
| P41226 | UBA7_HUMAN | 2.702535623 | 0.006881281 | O95571 | ETHE1_HUMAN | 12.99081696 | 0 |

**B.**

| Accession | UniprotID | Z test | Z test_pval |
|---|---|---|---|
| P10253 | LYAG_HUMAN | -16.05700874 | 0 |
| Q8NBJ7 | SUMF2_HUMAN | -11.3546636 | 0 |
| P60983 | GMFB_HUMAN | -8.375051083 | 0 |
| Q86VB7 | C163A_HUMAN | -7.260859905 | 3.84581E-13 |
| P27348 | 1433T_HUMAN | -6.910592649 | 4.82636E-12 |
| P08571 | CD14_HUMAN | -6.882265585 | 5.89084E-12 |
| P02792 | FRIL_HUMAN | -6.650279783 | 2.92537E-11 |
| Q9NUQ9 | FA49B_HUMAN | -6.62310143 | 3.51739E-11 |
| P19105 | ML12A_HUMAN | -6.599730501 | 4.11906E-11 |
| P07711 | CATL1_HUMAN | -6.547759984 | 5.84064E-11 |
| P06396 | GELS_HUMAN | -6.397107512 | 1.58348E-10 |
| P04233 | HG2A_HUMAN | -6.37871584 | 1.78579E-10 |
| P61970 | NTF2_HUMAN | -6.256460193 | 3.93814E-10 |
| P06865 | HEXA_HUMAN | -6.001931899 | 1.94983E-09 |
| P46926 | GNPI1_HUMAN | -5.916955254 | 3.27956E-09 |
| Q96CX2 | KCD12_HUMAN | -5.649376114 | 1.61031E-08 |
| P10619 | PPGB_HUMAN | -5.567933612 | 2.57778E-08 |
| Q9H4A4 | AMPB_HUMAN | -5.381559403 | 7.38433E-08 |
| P23229 | ITA6_HUMAN | -5.262997356 | 1.41726E-07 |
| O43567 | RNF13_HUMAN | -5.190502557 | 2.09727E-07 |
| P14174 | MIF_HUMAN | -5.098498339 | 3.42359E-07 |
| P04080 | CYTB_HUMAN | -5.080910183 | 3.75631E-07 |
| Q9NZZ3 | CHMP5_HUMAN | -5.054642881 | 4.31197E-07 |
| Q9H299 | SH3L3_HUMAN | -5.026662982 | 4.99088E-07 |
| Q16881 | TRXR1_HUMAN | -4.953443918 | 7.29114E-07 |
| P63208 | SKP1_HUMAN | -4.937754077 | 7.90274E-07 |
| P13686 | PPA5_HUMAN | -4.903474093 | 9.41564E-07 |
| Q9UBR2 | CATZ_HUMAN | -4.826173534 | 1.39181E-06 |
| P12270 | TPR_HUMAN | -4.801310499 | 1.57631E-06 |
| P15586 | GNS_HUMAN | -4.705258001 | 2.53545E-06 |
| P04406 | G3P_HUMAN | -4.65338436 | 3.26531E-06 |
| Q07954 | LRP1_HUMAN | -4.618940214 | 3.85705E-06 |
| P04066 | FUCO_HUMAN | -4.494476453 | 6.97413E-06 |
| P06733 | ENOA_HUMAN | -4.45419081 | 8.42102E-06 |
| P62328 | TYB4_HUMAN | -4.433105097 | 9.28856E-06 |
| P19971 | TYPH_HUMAN | -4.390342986 | 1.13172E-05 |
| P84103 | SRSF3_HUMAN | -4.317960691 | 1.57477E-05 |
| P00918 | CAH2_HUMAN | -4.265696088 | 1.9928E-05 |
| P15289 | ARSA_HUMAN | -4.258123299 | 2.0615E-05 |
| P00558 | PGK1_HUMAN | -4.227116934 | 2.36705E-05 |
| P09960 | LKHA4_HUMAN | -4.091783346 | 4.28068E-05 |
| O15031 | PLXB2_HUMAN | -4.08140049 | 4.47651E-05 |
| P02794 | FRIH_HUMAN | -4.062202652 | 4.86118E-05 |
| Q9H3G5 | CPVL_HUMAN | -4.055101413 | 5.01126E-05 |
| P01903 | DRA_HUMAN | -4.017401944 | 5.88433E-05 |
| P52209 | 6PGD_HUMAN | -3.853831512 | 0.000116284 |
| P14384 | CBPM_HUMAN | -3.749039048 | 0.000177513 |
| P29401 | TKT_HUMAN | -3.737489554 | 0.000185867 |
| P06280 | AGAL_HUMAN | -3.725041749 | 0.000195283 |
| P49721 | PSB2_HUMAN | -3.724089144 | 0.000196022 |
| P62995 | TRA2B_HUMAN | -3.661967233 | 0.000250286 |
| P30042 | ES1_HUMAN | -3.614417628 | 0.000301023 |
| P55008 | AIF1_HUMAN | -3.568568758 | 0.000358937 |
| O00754 | MA2B1_HUMAN | -3.567854524 | 0.000359916 |
| P25774 | CATS_HUMAN | -3.546892602 | 0.000389803 |
| Q06830 | PRDX1_HUMAN | -3.539565952 | 0.000400786 |
| Q12797 | ASPH_HUMAN | -3.494974377 | 0.000474107 |
| Q9NY15 | STAB1_HUMAN | -3.471224782 | 0.00051809 |
| O75368 | SH3L1_HUMAN | -3.398976672 | 0.000676385 |
| P16278 | BGAL_HUMAN | -3.371736402 | 0.000746959 |
| A6NL28 | TPM3L_HUMAN | -3.344562784 | 0.000824124 |
| P62308 | RUXG_HUMAN | -3.273341556 | 0.00106284 |
| P53634 | CATC_HUMAN | -3.241512007 | 0.001188974 |
| Q9UFN0 | NPS3A_HUMAN | -3.229154021 | 0.00124157 |
| O75340 | PDCD6_HUMAN | -3.224062946 | 0.001263856 |
| Q99497 | PARK7_HUMAN | -3.216682483 | 0.00129682 |
| P07602 | SAP_HUMAN | -3.190424405 | 0.00142064 |
| P23526 | SAHH_HUMAN | -3.17443375 | 0.001501292 |
| Q9BRK5 | CAB45_HUMAN | -3.158427842 | 0.001586226 |
| P20810 | ICAL_HUMAN | -3.153455765 | 0.001613497 |
| Q96SL1 | DIRC2_HUMAN | -3.152039858 | 0.001621341 |
| P56134 | ATPK_HUMAN | -3.122788913 | 0.001791462 |
| O00483 | NDUA4_HUMAN | -3.092897958 | 0.001982123 |
| Q9NY33 | DPP3_HUMAN | -3.084957223 | 0.002035814 |
| P38571 | LICH_HUMAN | -3.080526228 | 0.002066352 |
| P30479 | 1B41_HUMAN | -3.080257961 | 0.002068214 |
| P20674 | COX5A_HUMAN | -3.078359232 | 0.002081438 |
| P50395 | GDIB_HUMAN | -3.071185799 | 0.002132104 |
| O43852 | CALU_HUMAN | -3.054273457 | 0.002256063 |
| P60174 | TPIS_HUMAN | -3.049136992 | 0.002294998 |
| P22732 | GTR5_HUMAN | -3.014259973 | 0.00257607 |
| Q6P4A8 | PLBL1_HUMAN | -2.999768766 | 0.002701846 |
| P55957 | BID_HUMAN | -2.934833299 | 0.003337269 |
| P08575 | PTPRC_HUMAN | -2.93209541 | 0.003366833 |
| Q9BRF8 | CPPED_HUMAN | -2.928113613 | 0.003410254 |
| Q9UHA4 | LTOR3_HUMAN | -2.926679044 | 0.003426022 |
| P49189 | AL9A1_HUMAN | -2.894492876 | 0.003797715 |
| P14780 | MMP9_HUMAN | -2.894224481 | 0.003800963 |
| P07858 | CATB_HUMAN | -2.891324036 | 0.003836224 |
| Q9HB40 | RISC_HUMAN | -2.829247955 | 0.004665753 |
| P09211 | GSTP1_HUMAN | -2.819218649 | 0.004814071 |
| P37802 | TAGL2_HUMAN | -2.790170227 | 0.005268034 |
| Q9UNK0 | STX8_HUMAN | -2.767718881 | 0.005645013 |
| Q08170 | SRSF4_HUMAN | -2.767232154 | 0.005653448 |
| P00338 | LDHA_HUMAN | -2.766468246 | 0.00566671 |
| Q9HAV7 | GRPE1_HUMAN | -2.761463547 | 0.005754294 |
| P05107 | ITB2_HUMAN | -2.7217982 | 0.006492778 |
| O43504 | LTOR5_HUMAN | -2.709752813 | 0.006733337 |
| Q99873 | ANM1_HUMAN | -2.707391945 | 0.006781414 |
| P10599 | THIO_HUMAN | -2.67786824 | 0.007409236 |
| Q9NR45 | SIAS_HUMAN | -2.643982752 | 0.008193683 |
| P04229 | 2B11_HUMAN | -2.600311224 | 0.009313925 |
| Q10567 | AP1B1_HUMAN | -2.597993987 | 0.009377014 |
| P50897 | PPT1_HUMAN | -2.570550331 | 0.010153707 |
| Q96CM8 | ACSF2_HUMAN | -2.532894963 | 0.011312485 |
| P16949 | STMN1_HUMAN | -2.517804382 | 0.011808889 |
| O43707 | ACTN4_HUMAN | -2.506400663 | 0.012196732 |
| P53999 | TCP4_HUMAN | -2.493957693 | 0.01263276 |
| P01034 | CYTC_HUMAN | -2.484693744 | 0.012966293 |
| P60660 | MYL6_HUMAN | -2.476469349 | 0.013268902 |
| P09496 | CLCA_HUMAN | -2.466040472 | 0.01366159 |
| P35241 | RADI_HUMAN | -2.456938046 | 0.014012685 |
| P30273 | FCERG_HUMAN | -2.436034041 | 0.014849287 |
| Q16851 | UGPA_HUMAN | -2.418260766 | 0.015594897 |
| P20700 | LMNB1_HUMAN | -2.402257211 | 0.016294247 |
| O15144 | ARPC2_HUMAN | -2.395314241 | 0.016606126 |
| Q07812 | BAX_HUMAN | -2.384060864 | 0.01712277 |
| Q53GQ0 | DHB12_HUMAN | -2.383562581 | 0.017145969 |
| P08758 | ANXA5_HUMAN | -2.351666696 | 0.018689513 |
| Q9BUR5 | APOO_HUMAN | -2.346123087 | 0.018969842 |
| O14773 | TPP1_HUMAN | -2.334644153 | 0.019562018 |
| P06703 | S10A6_HUMAN | -2.328312221 | 0.019895531 |
| P47755 | CAZA2_HUMAN | -2.318056002 | 0.020446278 |
| Q96A26 | F162A_HUMAN | -2.298644087 | 0.021525158 |
| P62081 | RS7_HUMAN | -2.297948797 | 0.021564704 |
| P07686 | HEXB_HUMAN | -2.29228642 | 0.021889121 |
| Q14108 | SCRB2_HUMAN | -2.284458764 | 0.022344583 |
| P28066 | PSA5_HUMAN | -2.259539705 | 0.023849833 |
| P62158 | CALM_HUMAN | -2.257743607 | 0.023961649 |
| P26038 | MOES_HUMAN | -2.256252906 | 0.024054797 |
| P31150 | GDIA_HUMAN | -2.225244249 | 0.026064846 |
| Q9H2V7 | SPNS1_HUMAN | -2.210892258 | 0.027043299 |
| P05362 | ICAM1_HUMAN | -2.197422417 | 0.027990292 |
| P61163 | ACTZ_HUMAN | -2.195039647 | 0.028160754 |
| O43399 | TPD54_HUMAN | -2.19327613 | 0.02828749 |
| P42785 | PCP_HUMAN | -2.190892286 | 0.028459588 |
| P78417 | GSTO1_HUMAN | -2.17558923 | 0.029585989 |
| P30740 | ILEU_HUMAN | -2.149153429 | 0.03162224 |
| P13473 | LAMP2_HUMAN | -2.131544534 | 0.033044308 |
| O00233 | PSMD9_HUMAN | -2.127931352 | 0.033342776 |
| P08133 | ANXA6_HUMAN | -2.110211292 | 0.03484016 |
| P07195 | LDHB_HUMAN | -2.101090296 | 0.035633041 |
| O75821 | EIF3G_HUMAN | -2.098637016 | 0.035848911 |
| P07108 | ACBP_HUMAN | -2.094540603 | 0.03621185 |
| Q9UHL4 | DPP2_HUMAN | -2.092767962 | 0.036369873 |
| P27797 | CALR_HUMAN | -2.089269346 | 0.036683484 |
| P00738 | HPT_HUMAN | -2.08424168 | 0.037138189 |
| P49407 | ARRB1_HUMAN | -2.082518424 | 0.037295142 |
| P35237 | SPB6_HUMAN | -2.077856294 | 0.037722597 |
| P30101 | PDIA3_HUMAN | -2.046722129 | 0.040685375 |
| P20702 | ITAX_HUMAN | -2.0464082 | 0.040716226 |
| P04075 | ALDOA_HUMAN | -2.035295881 | 0.04182111 |
| P63220 | RS21_HUMAN | -2.02575854 | 0.042789534 |
| Q9HC38 | GLOD4_HUMAN | -2.018396415 | 0.043549992 |
| P05165 | PCCA_HUMAN | -2.015802933 | 0.043820587 |
| P62306 | RUXF_HUMAN | -2.007935672 | 0.044650128 |
| P15090 | FABP4_HUMAN | -2.004210389 | 0.045047528 |
| Q92688 | AN32B_HUMAN | -2.003537277 | 0.045119651 |
| P14618 | KPYM_HUMAN | -1.996792271 | 0.045847754 |
| Q9H7Z7 | PGES2_HUMAN | -1.993240777 | 0.046235088 |
| P30086 | PEBP1_HUMAN | -1.989992088 | 0.046591807 |
| P11279 | LAMP1_HUMAN | -1.985957279 | 0.047038068 |
| P67936 | TPM4_HUMAN | -1.978786996 | 0.047839993 |

**Figure S3. Differential protein profile of HIV-1 infected human MDM**. The quantitative expression of proteins identified from SWATH-MS (Z-test, $p < 0.1$) in HIV-1-infected human MDM is shown. The results were replicated in cells from four different donors. (A) Up-regulated and (B) down-regulated proteins in HIV-1 infected MDM 7 days after infection.

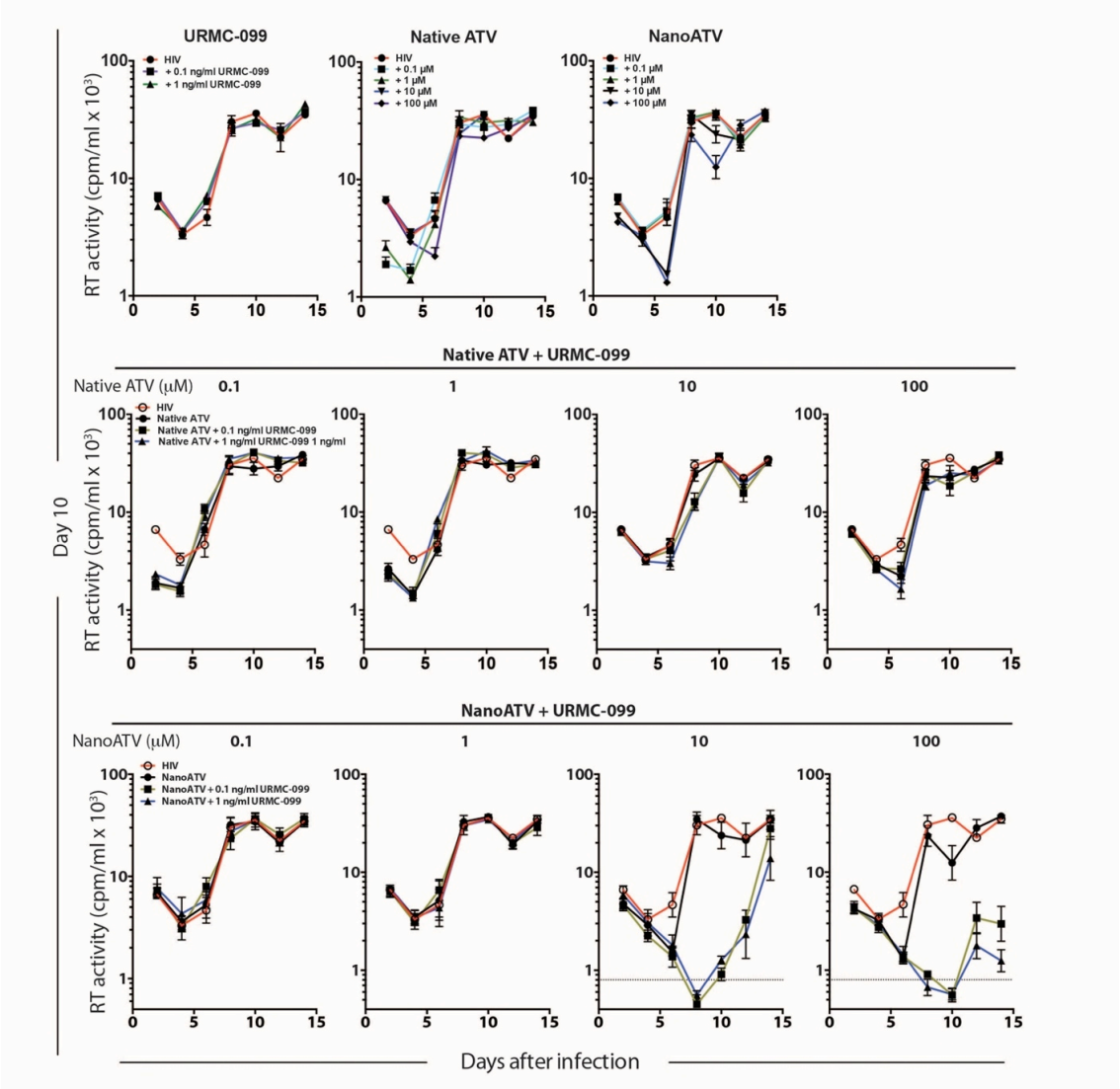


**Figure S4. URMC-099 enhanced nanoATV antiretroviral efficacy in HIV-1-infected human MDM.** MDM were treated with URMC-099 (0.1 or 1 ng/ml) and native ATV or nanoATV (100 $\mu$M) for 8 hours, cultured for an additional 10 days, then challenged with HIV-$1_{ADA}$ at 0.1 MOI. The infected MDM were maintained in medium with 0, 0.1 or 1 ng/ml URMC-099 for an additional 14 days. The cell culture medium was collected and assayed for HIV-1 RT activity. RT activity is expressed as mean $\pm$ SEM (n = 4). (A)

Native ATV or nanoATV or URMC-099 alone; (B) native ATV + URMC-099; (C) nanoATV + URMC-099.

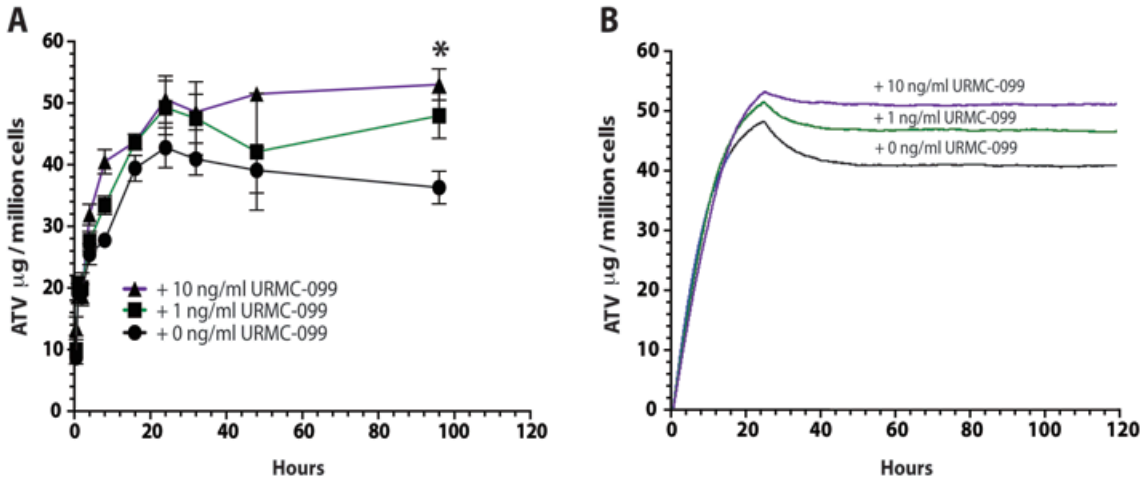


**Figure S5. URMC-099 enhanced nanoATV retention in MDM**. MDM were treated with 100 mM nanoATV for 24 hours. The treatment was removed and drug retention was determined over an additional 72 hours. (A) Time course of MDM uptake and retention of nanoATV in the presence of 0, 1 and 10 ng/ml of URMC-099 (black, green and purple, respectively), data are expressed as mean $\pm$ SEM (n=5). *Different from nanoATV + URMC-099 treatment compared with nanoATV alone, ($p < 0.05$, unpaired 2-tailed t test). (B) Mathematical simulation of the effect of URMC-099 on nanoATV uptake and retention in human MDM over 120 hours.

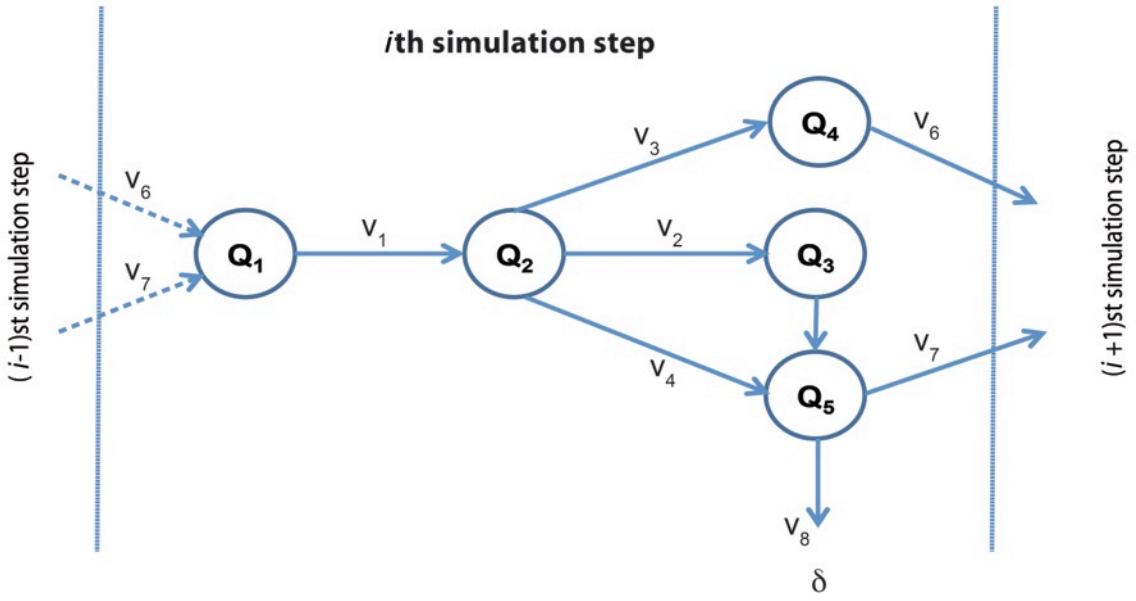


**Figure S6.** The modeled flow of nanoparticles is showing the simulation algorithm for the *i*th step with the major subcellular compartments involved in trafficking of nanoATV represented as the graph nodes $Q_2$, $Q_3$, $Q_4$, $Q_5$ and the cell's outside as $Q_1$. The values associated with $Q_1$, $Q_2$, $Q_3$, $Q_4$, $Q_5$ represent the concentrations of nanoATV or respective Rab proteins in a given simulation step. An open path marked δ in the schematic of Supplemental Fig. 6 corresponds to the decrease in time of the total number of the observed nanoATV particles. Time changes of the concentrations in the model are controlled by the set of five different equations:

$$Q_1^{(i)} = Q_1^{(i-1)} - V_1^{(i-1)}\Delta T + V_6^{(i-1)}\Delta T + V_7^{(i-1)}\Delta T$$

$$Q_2^{(i)} = Q_2^{(i-1)} + V_1^{(i-1)}\Delta T - V_2^{(i-1)}\Delta T - V_3^{(i-1)}\Delta T - V_4^{(i-1)}\Delta T$$

$$Q_3^{(i)} = Q_3^{(i-1)} + V_3^{(i-1)}\Delta T - V_6^{(i-1)}\Delta T$$

$$Q_4^{(i)} = Q_4^{(i-1)} + V_2^{(i-1)}\Delta T - V_5^{(i-1)}\Delta T$$

$$Q_5^{(i)} = Q_5^{(i-1)} + V_4^{(i-1)}\Delta T + V_5^{(i-1)}\Delta T - V_7^{(i-1)}\Delta T - V_8^{(i-1)}\Delta T$$

Where: $\Delta T$ denotes the time increment in simulations, and $(\cdot)^{(i)}$ denotes the value of $(\cdot)$ at *i*th step of simulation. The following relationships between the concentrations $Q_1, \ldots, Q_5$, and the rates of changes $V_1, \ldots, V_8$ were established from the experimental results using standard curve fitting methods implemented as standard MATLAB functions

$$V_1 = 0.3842Q_1 + 3.5$$

$$V_2 = 0.25Q_2 - 0.085Q_3 + 0.0814$$

$$V_3 = 0.55Q_2 - 0.30Q_4 + 2.238$$

$$V_4 = 0.003Q_1 + 0.42Q_2 - 0.18Q_3 - 0.36Q_5 + 0.75 + 0.495\alpha^{0.25}$$

$$V_5 = -0.003Q_1 + 0.18Q_3 - 0.33 - 0.495\alpha^{0.25}$$

$$V_6 = -0.0031Q_1 + 0.293Q_4 - 0.22 - 033\alpha^{0.25}$$

$$V_7 = -0.0031Q_1 + 0.036Q_5 - 0.112$$

$$V_8 = \frac{0.05}{1 + 0.125\alpha^{0.25}} \exp\left(\frac{0.05}{1 + 0.125\alpha^{0.25}} t\right) Q_5$$

where $\alpha$ is the concentration of URMC-099 in ng/mL, and *t* is time from the experiment start. The units for all the rates are $\mu$g/$10^6$ cells/hour and $\mu$g/$10^6$ cells for concentrations.

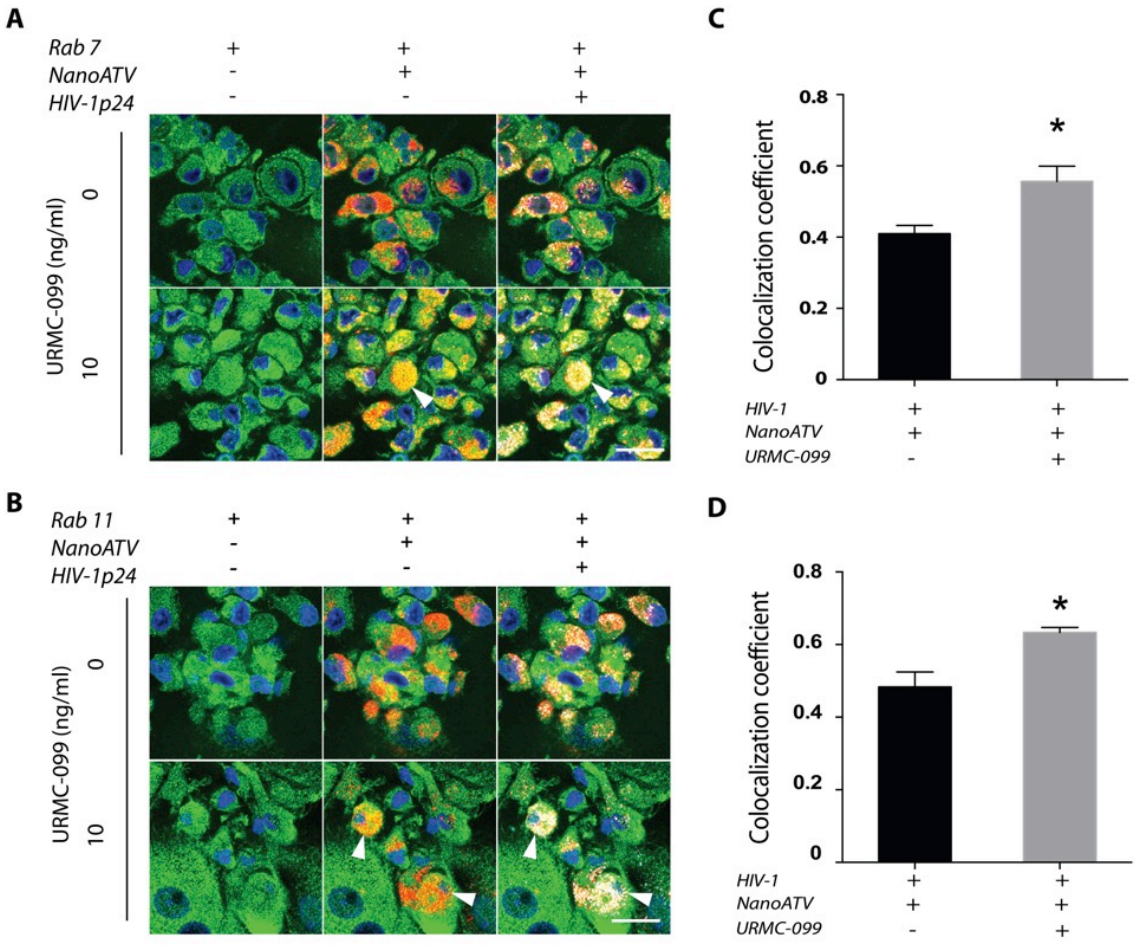


**Figure S7. URMC-099 affects accumulation of HIV-1p24 in subcellular compartments with nanoATV**. Human MDM were loaded with 100 $\mu$M CF568-labeled nanoATV (red) with or without 10 ng/ml URMC-099 for 16 hours and infected with HIV-$1_{ADA}$ at 0.1 MOI. After an additional 14 days in culture, MDM were fixed and immunostained with Rab7 (A) or Rab11 (B) antibody and AlexaFluor 488-labeled secondary antibody (green) and HIV-1p24 antibody and AlexaFluor 633-labeled secondary antibody. Arrowheads indicate overlap (yellow) of nanoATV and Rab compartments and overlap of nanoATV, Rab compartments and HIV-1p24 (white). DAPI (blue) stain indicates cell nuclei, 1260X magnification. Percent overlap of HIV-1p24,

nanoATV and Rab7 (C) or Rab11 (D) compartment was quantitated. Data are expressed as average $\pm$ SEM, n=30 ($p < 0.05$, unpaired 2-tailed t test). Scale bar equals 20 $\mu$m.